ISSN (print): 1698-6180. ISSN (online): 1886-7995
www.ucm.es/info/estratig/journal.htm

Journal of Iberian Geology 36 (1) 2010: 21-38

Journal of Iberian Geology
AN INTERNATIONAL PUBLICATION OF EARTH SCIENCES

Recent tectonic and morphostructural evolution of Byers Peninsula (Antarctica): insight into the development of the South Shetland Islands and Bransfield Basin

Evolución tectónica y morfoestructural reciente de la Península Byers (Antártida): evidencias sobre el desarrollo de las Islas Shetland del Sur y la Cuenca de Bransfield

P. Alfaro*[1], J. López-Martínez[2], A. Maestro[2,3], J. Galindo-Zaldívar[4], J.J. Durán-Valsero[3], J.A. Cuchí[5]

[1]*Departamento de Ciencias de la Tierra y del Medio Ambiente. Universidad de Alicante, Apdo. 99, 03080 Alicante, Spain. pedro.alfaro@ua.es*
[2]*Departamento de Geología y Geoquímica. Universidad Autónoma de Madrid. 28049 Madrid, Spain. jeronimo.lopez@uam.es*
[3]*Instituto Geológico y Minero de España, Ríos Rosas, 23. 28003 Madrid, Spain. a.maestro@igme.es; jj.duran@igme.es*
[4]*Departamento de Geodinámica. Universidad de Granada. IACT. 18071 Granada, Spain. jgalindo@ugr.es*
[5]*Escuela Politécnica Superior de Huesca. Universidad de Zaragoza. Carretera de Cuarte s/n, 22071 Huesca, Spain. cuchi@unizar.es*

**Corresponding author*

Received: 22/12/09 / Accepted: 25/01/10

Abstract

Byers Peninsula forms the western extremity of the Livingston Island (Antarctica) in the continental South Shetland Block. This tectonic block is bounded by the South Shetland Trench to the north, the Bransfield back-arc basin to the south, and extends to the South Scotia Ridge on the east. Westwards it is connected to the Antarctic Plate by a broad deformation zone located at the southern end of the Hero Fracture Zone. In Byers Peninsula we analyzed more than 1,200 lineaments, and 359 fault planes from 16 sites, both in sedimentary and intrusive igneous rocks. Statistical analysis of lineaments and mesoscopic fractures, with a length varying between 31 and 1,555 m, shows a NW-SE maximum trend, with two NE-SW and ENE-WSW secondary maximums. Fault orientation analysis shows similar trends suggesting that most of the lineaments correspond to fractures. Due to the absence of striated faults and the lack of kinematic evidence on the regime in most of the analyzed faults we have used the Search Grid paleostress determination method. The results obtained allow us to improve and complete the data on the recent evolution of the South Shetland Block. In this complex geodynamic setting, Byers Peninsula has been subjected to NNW-SSE to NNE-SSW extension related to Bransfield Basin

opening and NE-SW and NW-SE local compressions respectively associated to Scotia-Antarctic plate convergence and the South Shetland Trench subduction.

Keywords: Antarctica, Byers Peninsula, mesostructural analysis, morphotectonics, paleostress, South Shetland Islands.

Resumen

La Península Byers se localiza en el extremo occidental de la Isla Livingston (Antártida) que pertenece al bloque continental de las Shetland del Sur. Este bloque tectónico está limitado al norte por la Fosa de las Shetland del Sur, al sur por la cuenca de trasarco de Bransfield, y hacia el este se extiende por la Dorsal Sur de Scotia. Hacia el oeste conecta con la placa Antártica a través de una amplia zona de deformación localizada en la prolongación meridional de la Zona de Fractura Hero. En este trabajo se han analizado conjuntamente más de 1.200 lineamientos, así como 359 planos de fallas en 16 estaciones en rocas sedimentarias e ígneas de la Península Byers. El análisis estadístico de los lineamientos y las fracturas a escala mesoscópica, con una longitud que oscila entre 31 y 1.555 m, muestran una orientación máxima NO-SE, con dos máximos secundarios de dirección NE-SO y ENE-OSO. El análisis de las fracturas muestra orientaciones similares que sugieren que gran parte de estos lineamientos están relacionados con fracturas. La ausencia de indicadores cinemáticos de calidad en la mayor parte de las fracturas sólo nos ha permitido aplicar el método de Redes de Búsqueda para el cálculo de paleoesfuerzos. Los resultados obtenidos son compatibles con los obtenidos en otros sectores del Bloque de las Shetland del Sur. En este complejo contexto geodinámico, la Península Byers ha estado sometida a extensión NNW-SSE/ NNE-SSW ligada a la apertura de la cuenca de Bransfield, así como a compresión local NE-SO y NO-SE asociada respectivamente a la convergencia entre las placas Scotia y Antártica, y a la subducción en la Fosa de las Shetland del Sur.

Palabras clave: Antártida, Península Byers, análisis mesoestructural, morfotectónica, paleoesfuerzos, Islas Shetland del Sur

1. Introduction

Byers Peninsula, located in the westernmost part of Livingston Island (South Shetland Islands), is the largest ice free area in the South Shetland Archipelago and constitutes an interesting place to study the recent tectonic evolution of the South Shetland Block. This continental fragment of the southern branch of the Scotia Arc is bordered by active deformation zones (Fig 1): the South Shetland Trench to the north, the Bransfield back-arc basin to the south, and extends eastwards along the South Scotia Ridge. Westwards it is connected to the Antarctic Plate by a broad deformation zone located at the southern prolongation of the Hero Fracture Zone.

The region has had a complex geodynamic evolution because it has been influenced by the extension related to the opening of the Bransfield Basin (Barker *et al.*, 1991), the left-lateral displacement of the Scotia and Antarctic plates along the transtensional fault zone that extends along the South Scotia Ridge (Galindo-Zaldívar *et al.*, 1996, 2004), and the subduction of the Phoenix Plate under the Antarctic Plate that progressively ends north-eastwards along the Pacific margin of the Antarctic Peninsula (Dalziel, 1983) (Fig. 1). Therefore, rocks of Byers Peninsula have been subject to different regional geodynamic processes.

Several geological studies have been carried out in Byers Peninsula, mainly focused on stratigraphy and paleontology (e.g. Smellie *et al.*, 1980, Crame *et al.*, 1993), petrology (e.g. Hobbs, 1968, Smellie *et al.*, 1984; Demant *et al.*, 2004) and geomorphology (e.g. López-Martínez *et al.*, 1996a). There are not specific studies on palaeostress analysis in the study area. This paper is focused on the integration of morphostructural data and brittle mesostructural analysis. We made a paleostress analysis showing stress tensors that were related to the recent tectonic evolution that produced brittle structures. Results are compared with others obtained in Livingston Island, different areas of the South Shetland Islands and the Antarctic Peninsula. Finally, the local stress regime estimated for Byers Peninsula is integrated in the regional geodynamic models proposed for the region.

2. Geological context

2.1. Regional tectonic setting

Byers Peninsula (Livingston Island) is included in the South Shetland Block, a Jurassic-Quaternary magmatic forearc generated by Mesozoic and Cenozoic subduction processes along the South Shetland Trench (Smellie *et al.*, 1984). More specifically, Byers Peninsula is located along the segment between the Former Phoenix Plate and the Antarctic Plate, bounded by the Shackleton and Hero Fracture zones (Fig. 1). This segment, bounded to the north by the South Shetland Trench, is presently characterized by active subduction, according to most authors (Gamboa and Maldonado, 1990; Larter and Barker, 1991, Maldonado *et al.*, 1994). Nevertheless, other studies indicate that convergence of the oceanic Phoenix and Antarc-

tic plates concluded about 4Ma ago (Barker *et al.*, 1991).

In this geodynamic context, the southern border of Livingston Island is characterized by longitudinal E-NE trending faults, which are responsible for the relative uplift of the South Shetland Block. High-angle normal faults constitute the southern boundary of the tectonic horst (González-Casado *et al.*, 1999, Galindo-Zaldívar *et al.*, 2004). Uplift has been attributed to different causes such as the emplacement of Tertiary plutonic intrusions (Ashcroft, 1972), or to passive subduction of the former Phoenix Plate and rollback of the South Shetland Trench (e.g. Smellie *et al.*, 1984; Maldonado *et al.*, 1994; Lawver *et al.*, 1995, 1996). Another mechanism proposed was the sinistral trans-tensional movement between the Antarctic and Scotia plates causing oblique extension along the Antarctic Peninsula continental margin generating the Bransfield Basin and defining the South Shetland tectonic block (e.g. Rey *et al.*, 1995; Klepeis and Lawver, 1996; Lawver *et al.*, 1996; González Casado *et al.*, 2000; Galindo-Zaldívar *et al.*, 2004; Maestro *et al.*, 2007; Solari *et al.*, 2008). The opening rate of Bransfield Basin seems to have accelerated from 1.1 mm/yr during Oligocene-Miocene (Sell *et al.*, 2004) to 2.5-7.5 mm/yr for the last 2 Ma (González-Ferrán, 1991).

The present geodynamic setting of the region can be investigated by seismotectonic and geodetic studies. Stress orientations deduced from earthquake focal mechanisms and fault analysis is related to a sinistral movement between the Antarctic and Scotia plates (Pelayo and Wiens, 1989; Galindo-Zaldivar *et al.*, 1996; González-Casado *et al.*, 2000). Geodetic data show that Bransfield Basin is opening at 5-20 mm/yr in a NW-SE direction (Dietrich *et al.*, 1996). In addition, the South Shetland Block moves 17 mm/yr in a N020E direction with respect to the Antarctic Plate (Dietrich *et al.*, 2001).

2.2. Geology of Byers Peninsula

Hobbs (1968) carried out the first reconnaissance work in 1957-58. Several papers contain geological maps of all parts of Byers Peninsula (Hobbs, 1968; Valenzuela and Hervé, 1972; Pankhurst *et al.*, 1979; Smellie *et al.*, 1980). Early studies covered the paleontology and general stratigraphy of the area (Araya and Hervé, 1966; González Ferrán *et al.*, 1970; Tavera, 1970; Hernández and Azcárate, 1971; Valenzuela and Hervé, 1972; Covacevich, 1976). Smellie *et al.* (1980, 1984) proposed a stratigraphic subdivision of the Mesozoic rocks of Byers Peninsula. This was revised and updated by Crame *et al.* (1993) and by Hathway and Lomas (1998).

The Byers Peninsula includes a succession of Upper Jurassic-Lower Cretaceous sedimentary deposits assigned to the Byers Group (Smellie *et al.*, 1984; Crame *et al.*, 1993) (Fig. 2). This is a thick sedimentary sequence

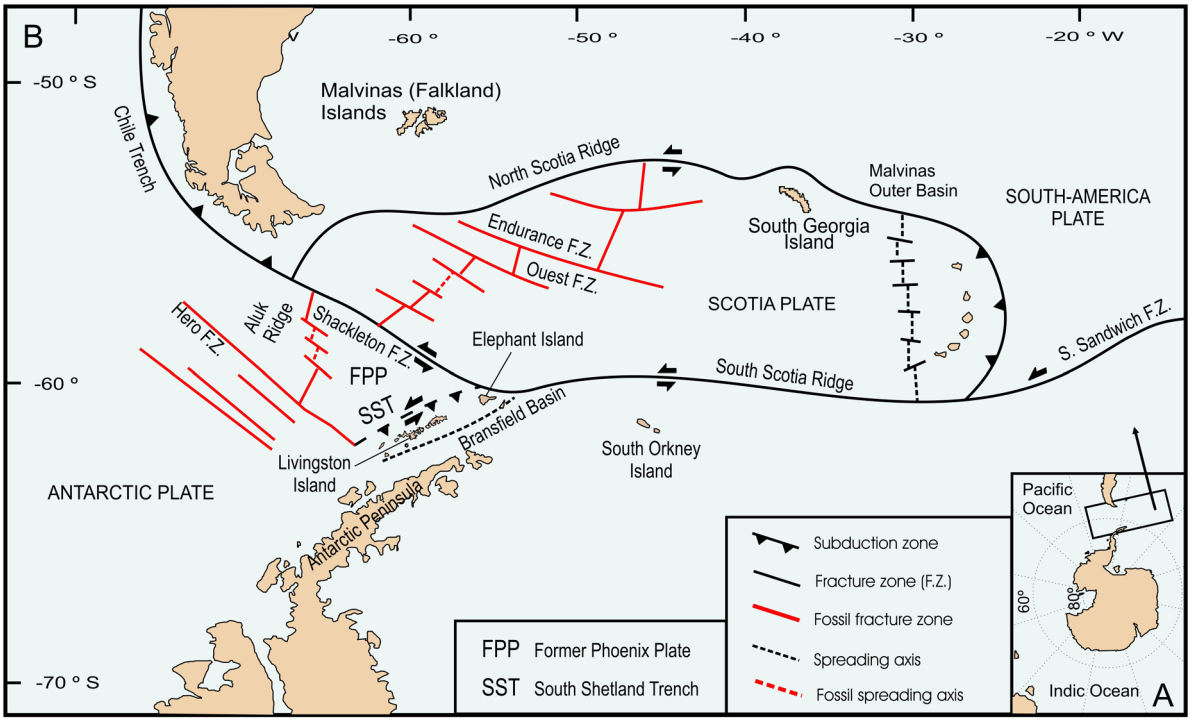

Fig 1.- Regional tectonic framework of the Scotia Arc and northwestern Antarctic Peninsula regions.
Fig. 1.- Marco tectónico regional del Arco de Scotia y del sector septentrional de la Península Antártica.

characterized by over 1 km of marine clastic rocks, unconformably overlain by 1.4 km of non-marine volcanoclastic strata (Smellie *et al.*, 1984; Crame *et al.*, 1993; Hathway and Lomas, 1998). According to Hathway and Lomas (1998), the sedimentary sequence cropping out on Byers Peninsula (also in Rugged Island and President Head on Snow Island) is composed, from bottom to top, of the Anchorage Formation (Kimmeridgian-Tithonian), the President Beaches Formation and the Start Hill Formation (Berriasian), the Chester Cone Formation (Upper Berriasian to Valanginian) and the Cerro Negro Formation (early Aptian). Hathway and Lomas (1998) indicated an equivalence of these Formations with those previously proposed by Smellie *et al.* (1980) and Crame *et al.* (1993). Penecontemporaneous intrusive igneous rocks (mainly sills, dykes and plugs of basalt-basaltic andesite composition) are present in much of the succession (Smellie *et al.*, 1980), especially in the marine strata (Fig. 2).

In a regional study, Smellie *et al.* (1980) carried out the first tectonic study of Byers Peninsula. They described several faults and folds, but focused on the dyke trends and their relationship with faults. In general, Smellie *et al.* (1984) assumed that most of the faults and dykes are not much younger than their host rocks. The dykes of Byers Peninsula have a wide range of orientations concentrated toward the SE to ESE (López-Martínez *et al.*, 1996a).

Quaternary deposits and landforms are extensively exposed on Byers Peninsula. The general morphology of the Peninsula is dominated by a series of raised marine platforms and beaches at different altitudes, as well as, a well developed drainage network including temporary streams and many lakes and ponds (López-Martínez *et al.*, 1996b).

3. Methods

Palaeostress analysis was conducted on fault planes, measured at 16 sites in Mesozoic rocks of Byers Peninsula (Fig. 2). Most sites are in intrusive rocks but four sites are located in sedimentary rocks. A total of 359 faults have been measured and analyzed. The slip on the normal fault planes varies between centimeters and a few meters, whereas the slip measured on reverse faults was only a few centimeters (Fig. 3). Slickenlines and chatter marks on the fault surfaces are scarce due to rock properties.

We used a method of stress inversion described by Galindo-Zaldivar and González-Lodeiro (1988) for situations in which some slip-sense indicators are lacking. This is named Search Grid Inversion Paleostress Determination method, and provides data on the main axis orientation and the axial ratios of the stress ellipsoids. This method tries to justify as many as possible of the measured faults with the minimum number of overprinted stress ellipsoids, using a systematic search on a grid and involves striae from both known and unknown fault regimes. At the sites were there is lack of fault regime determinations in all of the measures, the method provides two alternative stress ellipsoids for each faulting stage that corresponds to the two possible opposite fault regimes of each fault .

Photointerpretation of vertical aerial photographs obtained in December 1956 and February 1957 (Falkland Islands and Dependencies Aerial Survey expedition) shows several linear elements on the Byers Peninsula. Some of these are reflected in the topography (CGE-UAM-BAS, 1992) by relief features (e.g. contour patterns or coastline). Other linear elements are faults or dykes, but most are composite features, including structurally controlled streams, lake lineaments, scarps and cliffs (López-Martínez *et al.*, 1995).

The high number of lineaments identified (1,259) made necessary to use an automatic exploration program for the determination of some of their characteristics. This program reads vectorial files (DXF in our case) and explores systematically first along the X-axis and then along the Y-axis. This program generates a file that provides, among other results, the length of each line and its orientation. From these data, different conventional statistical programs were used for the analysis of lineaments.

Lineament distribution is shown here as density fracture maps. These maps are built making a net of square cells and calculating the length of the lines contained within the individual cell limits. The result is divided by the cell area. From the data file containing the coordinates of the beginning and end of each fracture, the program calculates the number of fractures beginning or ending within each cell. Nevertheless, an automatic computation program is necessary to determine the length of lineaments or the length of segments of lineaments included within each cell (program LINDENS by Casas *et al.,* 2000).

The elaboration of density maps begins with the determination of the most appropriate cell size. The critical size of the grid is conditioned by the average size of the lineaments and the distance between them. To determine these distances, the Delaunay triangulation method (Preparata and Shamos, 1985) was applied. Each fracture is represented by its middle point. The vertices of Delaunay's triangles are constituted by these middle points. The distance from each lineament (point) to its two nearest neighbours is then calculated. The average distance between three lineaments is considered as the arithmetic

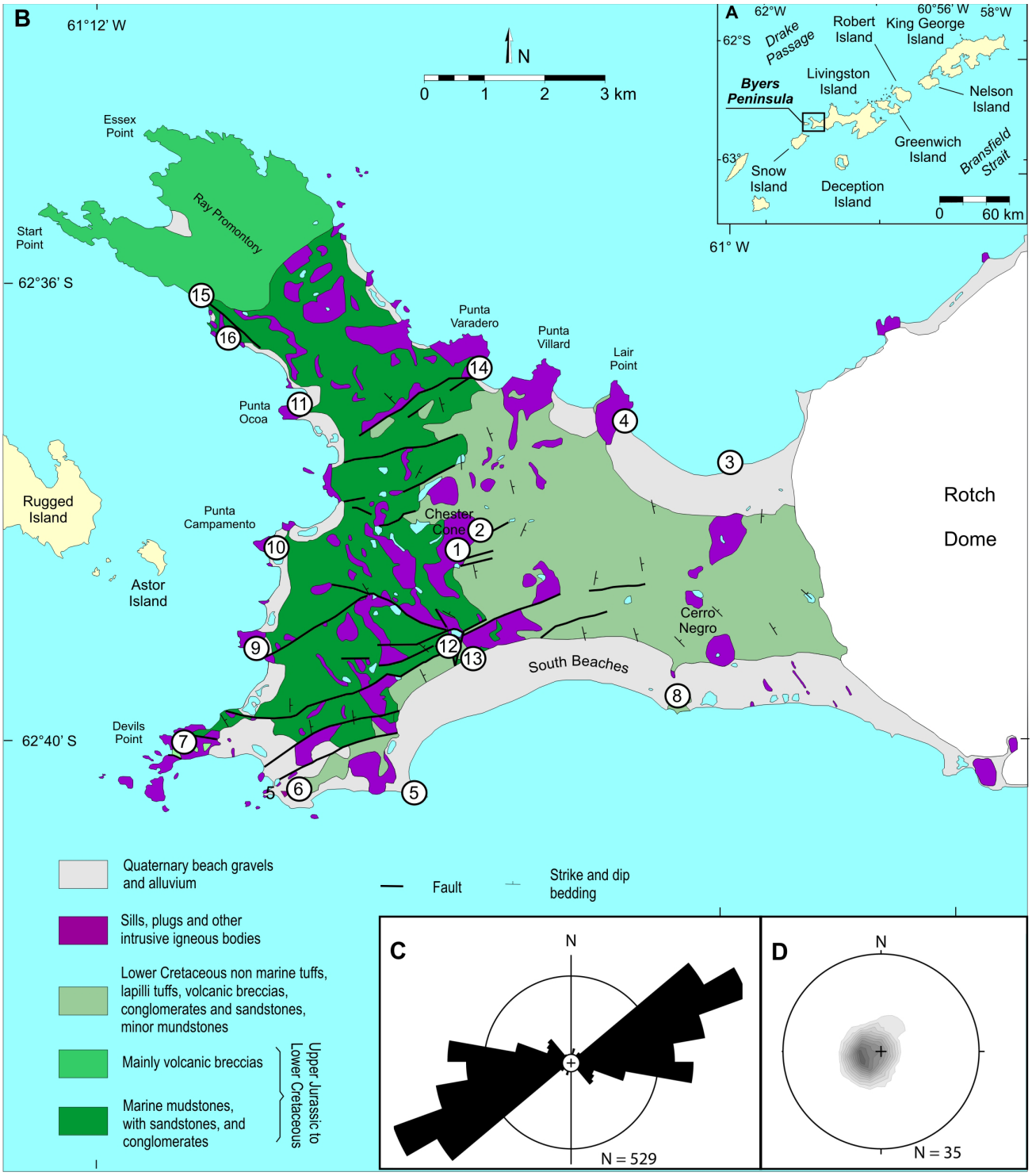

Fig. 2.- A) Location of Byers Peninsula in the South Shetland Islands. B) Simplified geological map of Byers Peninsula (after López-Martínez *et al.*, 1996) and location of the studied fracture sites. C) Rose diagram of macroscopic fault orientation, with weighted fracture trace length (combined with data from López-Martínez *et al.* (1995, 1996a). Outer circle represents 10%. D) Density stereoplots representing the bedding pole obtained from recompilation data of sedimentary Cretaceous units from López-Martínez *et al.* (1995) and this study. Equal area projection, lower hemisphere. Contour interval 2%.

Fig. 2.- A) Localización de la Peninsula Byers en el contexto de las Islas Shetland del Sur. B) Mapa geológico simplificado de la Penisula Byers (López-Martínez *et al.*, 1996) y localización de las estaciones de fracturas analizadas. C) Diagrama en rosa de la orientación ponderada de las fallas de escala macroscópicas cartografiadas en la Península Byers por López-Martínez *et al.* (1995, 1996a). El círculo externo representa el 10% de los datos. D) Representación estereográfica de la densidad de los polos de estratificación de las unidades sedimentarias cretácicas obtenidos a partir de datos del trabajo de López-Martínez *et al.* (1995) y del estudio de campo llevado acabo para realizar este trabajo. Proyección equiareal, hemisferio inferior. Intervalo de contorno 2%.

mean of the three sides of the triangle, and plotted at the centre of each triangle. This process is achieved by means of an automatic program (TRIANGLE, by J. Bernal, unpublished) which calculates the arithmetic mean of the three sides of each triangle. To appreciate the variations of this distance and the most representative distances from their distribution over the area, a contour map of average distances between lineaments was drawn.

4. Results of the analysis of lineaments and brittle mesostructures

4.1 Paleostress analysis from brittle mesostructures

We have analyzed faults at 16 sites in Byers Peninsula in Mesozoic rocks of the Byers Group. Most of the sites are located along the peninsula coast. At the north coast, site 3 is located at the north beach next to Rotch Dome, site 4 at Lair Point and site 14 at Punta Varadero, all of them in igneous intrusive rocks. Four sites (5, 6, 7 and 8) are located along the south coast, between the SW of Cerro Negro and Devils Point. They are located in igneous rocks except site 6 which is located in volcanoclastic rocks of the Cerro Negro Formation. Along the western coast, between Devils Point and Start Point, sites 9 and 15 are located in mudstones of the President Beaches Formation, while sites 10, 11 and 16 are located in igneous rocks. At the center of the peninsula, sites 1 and 2 are located in igneous rocks of the Usnea Plug and Chester Cone respectively. Finally, sites 12 and 13 are located respectively along a stream which flows into the South Beaches, in sedimentary rocks of the Chester Cone

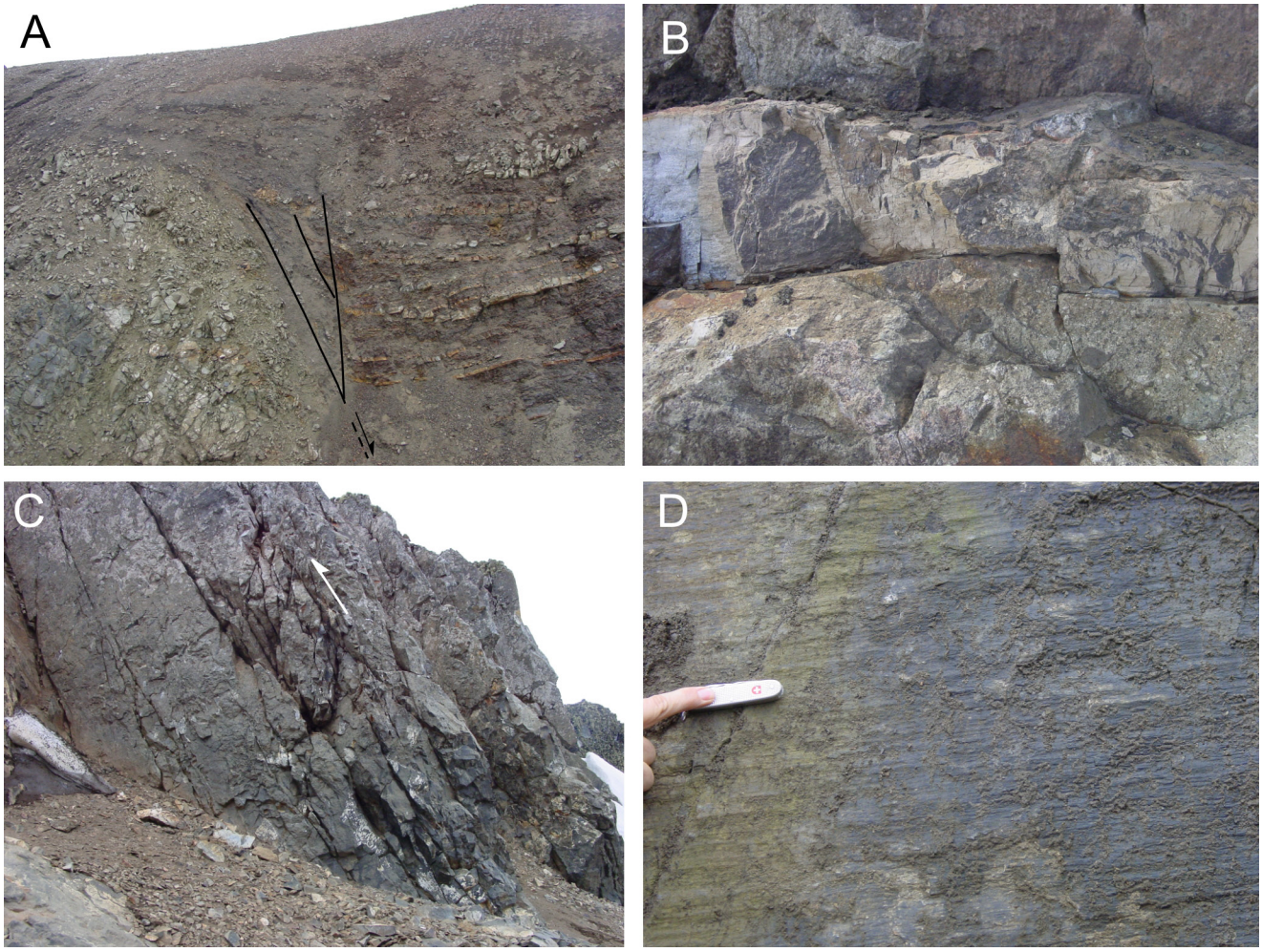

Fig. 3.- Examples of the brittle structures analyzed in this study. A. Metric-scale normal fault zone between intrusive igneous rocks and Mesozoic rocks of Byers Group, south of Punta Varadero (site 14). B. Faults have centimetric scale offsets (sedimentary rocks of site 9, western coast). C. Sigmoidal structures observed at site 8, next to Cerro Negro. D. Detail of a striated fault plane at site 10, Punta Campamento.

Fig. 3.- Ejemplos de estructuras frágiles analizadas en este estudio. A. Falla normal de escala métrica entre rocas ígneas intrusivas y rocas Mesozoicas del Grupo Byers, al sur de Punta Varadero. B. Fallas de salto centimétrico (rocas sedimentarias de la estación 9, en la costa occidental). C. Estructuras sigmoidales en la estación 8, en las proximidades de Cerro Negro. Detalle de un plano de falla estriado en la estación 10, Punta Campamento.

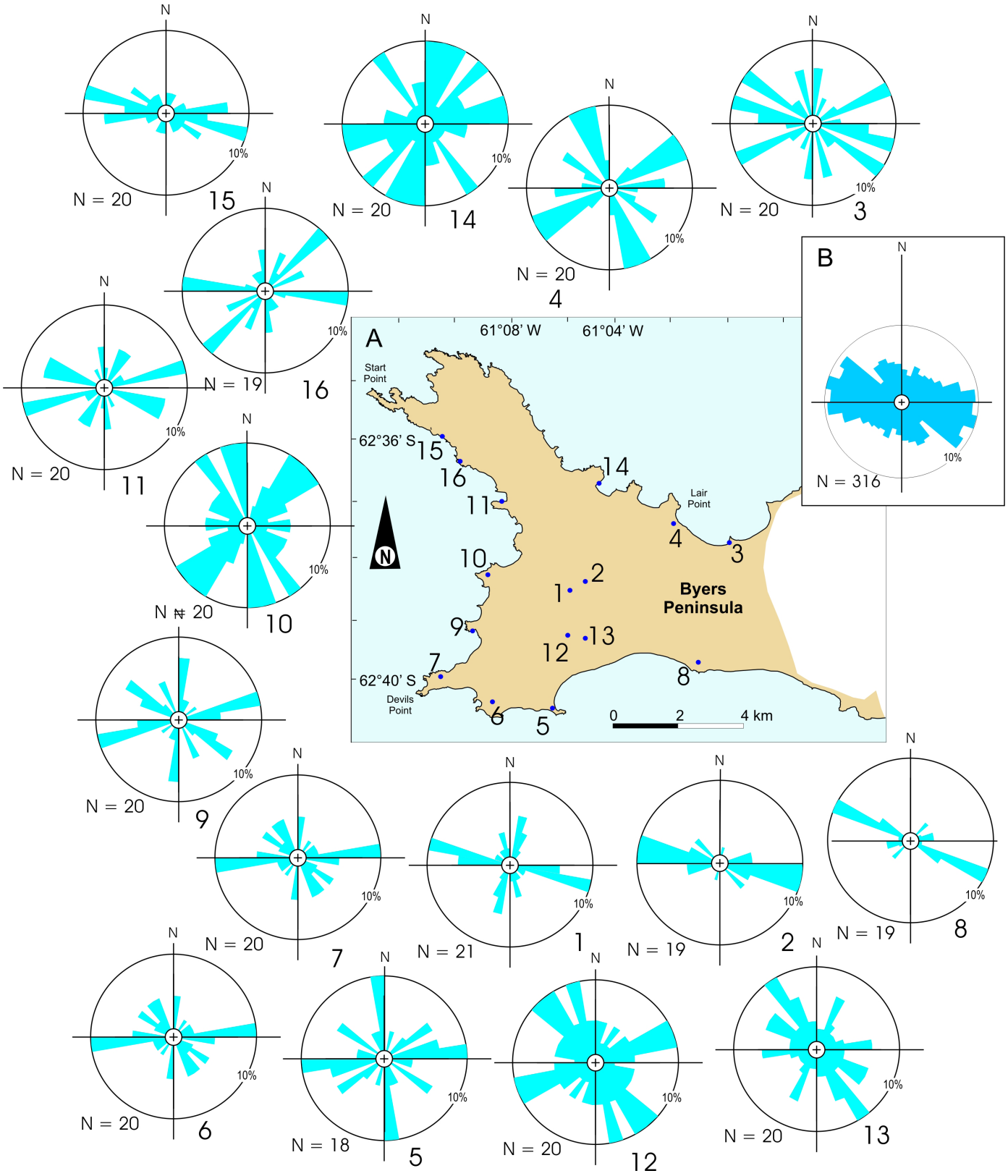

Fig. 4.- A) Location of study sites in Byers Peninsula. Rose diagrams of orientation of faults at the outcrop scale (outer circle represents 10%). N: Number of data; see Table I. B) Rose diagram indicating the orientation frequency for all measured faults (outer circle represents 10%).

Fig. 4.- A) Localización de las estaciones analizadas en la Península Byers. Se muestra los diagramas en rosas de las orientaciones de fallas medidas (el circulo externo representa el 10%). N: número de datos, ver Tabla I. B) Diagrama en rosa indicando la frecuencia de orientaciones de todas las falla medidas (el circulo externo representa el 10%).

Site	Lithology	So (strike/dip)	Most probable			R axial ratio
			σ_1 (plunge/ strike)	σ_2	σ_3	
1	Igneous		16/354	29/094	56/239	0.05
			58/224	30/067	10/331	0.08
2	Igneous		20/258	40/005	44/148	0.12
3	Igneous		20/098	68/248	10/004	0.03
4	Igneous		20/105	70/297	04/196	0.49
			62/049	18/176	21/273	0.48
5	Igneous		33/296	53/149	16/037	0.15
6	Cerro Negro Fm	N70E 20NW	18/044	70/199	08/311	0.09
			14/205	70/339	14/111	0.48
7	Igneous		08/131	16/039	72/246	0.09
			32/095	58/271	02/004	0.35
8	Igneous		72/192	04/090	18/359	0.01
9	President Beaches Fm	N115E 18SW	09/310	28/045	60/204	0.21
10	Igneous		08/302	02/212	82/108	0.29
11	Igneous		06/000	20/268	69/106	0.01
12	Chester Cone Fm	N98E 24NW	04/072	26/340	64/170	0.35
13	Igneous		77/350	10/131	08/222	0.06
14	Igneous		06/082	12/173	77/326	0.23
15	President Beaches Fm	N124E 25SW	76/294	02/032	14/122	0.06
			66/158	15/286	18/021	0.11
16	Igneous		15/251	16/157	68/021	0.49
			16/201	00/291	74/021	0.46

Table I.- Summary of stress tensors and stress orientations obtained from fault population analysis. Sites are located in figure 2; Formation name; So bedding orientation in site, strike/dip;σ_1, σ_2 and σ_3 values of principal stress axes; R stress ratio = $(\sigma_2–\sigma_3)/(\sigma_1–\sigma_3)$ (Wallace, 1951).

Tabla I.- Resumen de los tensores y orientaciones de esfuerzo obtenidos a partir del análisis poblacional de fallas. Las estaciones están localizadas en la figure 2; nombre de la Formación; So: estratificación en la estación, dirección/buzamiento; G1, G2 y G3: valores de los ejes principales de esfuerzo; R relación de esfuerzos = $(\sigma_2–\sigma_3)/(\sigma_1–\sigma_3)$ (Wallace, 1951).

Formation and in igneous rocks (Fig. 2).

The structures studied at outcrop scale are different types of faults with offsets from centimetric to as much as a few meters. The methodology for the quantitative study of orientation is based on the definition of different fracture sets and a determination of the dominant direction in each exposure (16 sites in total and 359 surface faults). The fracture orientation data are displayed by means of rose diagrams (Fig. 4). Overall, faults at the outcrop scale show a WNW-ESE orientation maxima. Although some of them show well developed striae, it is difficult to determine the fault regime in most of the cases owing to the poor exposure of these markers. Observed fault regimes are variable: some of them correspond to normal faults (20), reverse faults (9) and strike-slip faults (25). Joints, most of them with vertical planes, are not included in this study.

The results of the paleostress analysis are summarized in Table 1 and they have been represented in figure 5. Stress tensors are defined as orientations of the most probable main axes (σ_1, σ_2 and σ_3) and the stress ratio ($R= (\sigma_2 - \sigma_3) / (\sigma_1 - \sigma_3)$). Orientations of σ_1 show two main axes trending NE-SW and NW-SE, whereas the σ_3 direction is NNW-SSE to NNE-SSW. At the outcrop scale, the relative chronology between extensional and compressional structures is not always clear.

The results obtained using this method indicate the existence of overprinted deformations on the Byers Peninsula because, in most of the measurement sites, two fault stages have been established. Most of the calculated faulting stages corresponds to stress ellipsoids characterized by a main axis (odd-axis) with a magnitude very different to the other two main axes. The odd axis corresponds to the maximum well defined compression in prolate ellipsoids or the well constrained extension in oblate ellipsoids. In stations 4, 6 and 16 the stress ellipsoids have axes with different magnitudes. The odd axes show very regular orientations in the different sectors of the region supporting the hypothesis that Byers Peninsula has

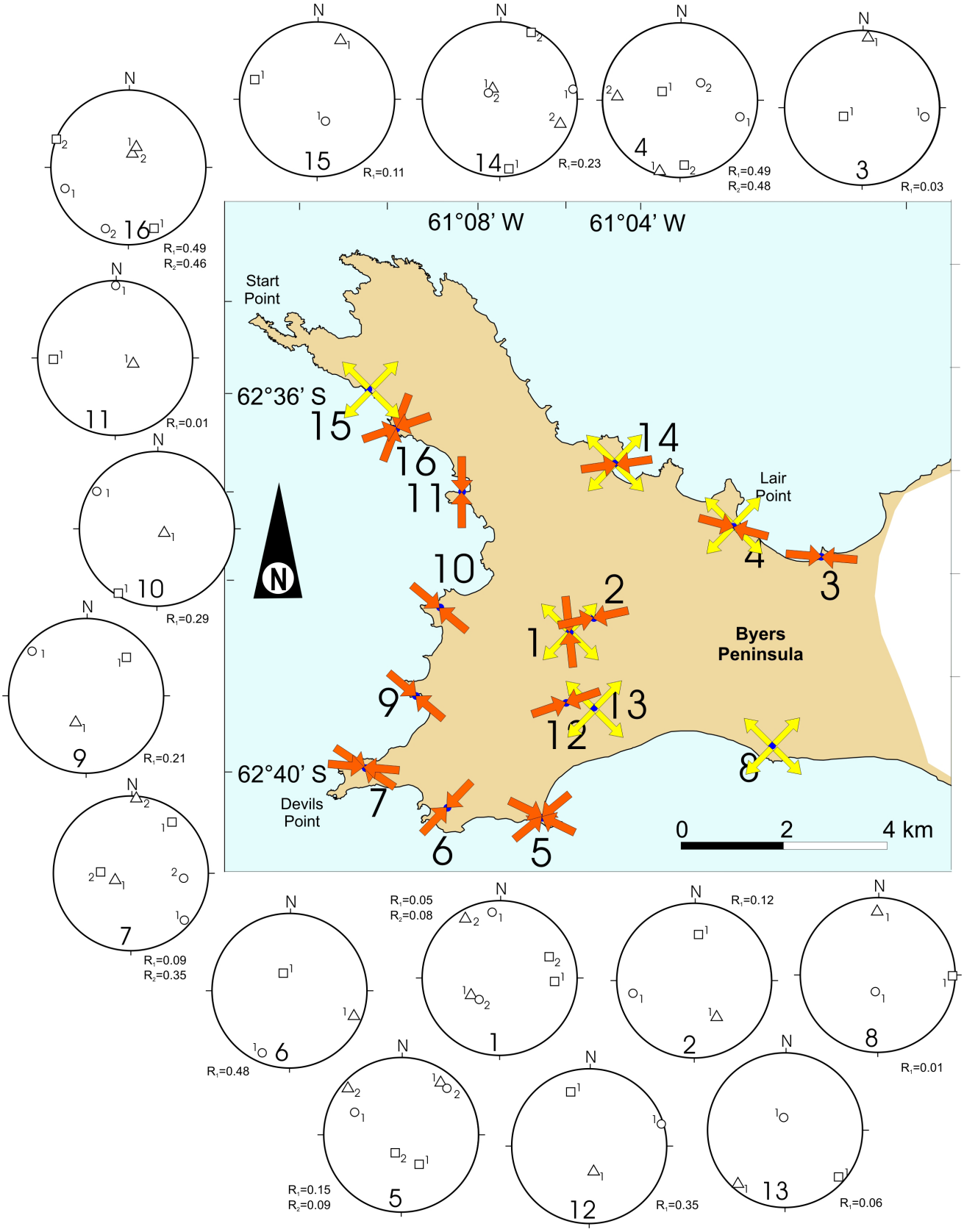

Fig. 5.- Location of study sites in Byers Peninsula. Stereoplots include stress axes (σ_1: white circle, σ_2: white square, and σ_3: white triangle). R stress ratio = $(\sigma_2-\sigma_3)/(\sigma_1-\sigma_3)$. N: Number of data; see Table I. Arrows show σ_1 and σ_3 directions obtained from paleostress analysis.

Fig. 5.- Localización de las estaciones analizadas en la Península Byers. Se muestra la representación estereográfica de los ejes de esfuerzos (σ_1: circulo blanco, σ_2: cuadrado blanco, y σ_3: triangulo blanco). R relación de esfuerzos = $(\sigma_2-\sigma_3)/(\sigma_1-\sigma_3)$. N: número de datos, ver Tabla I. Las flechas indican las direcciones de σ_1 y σ_3 obtenidas a partir del análisis de paleoesfuerzos.

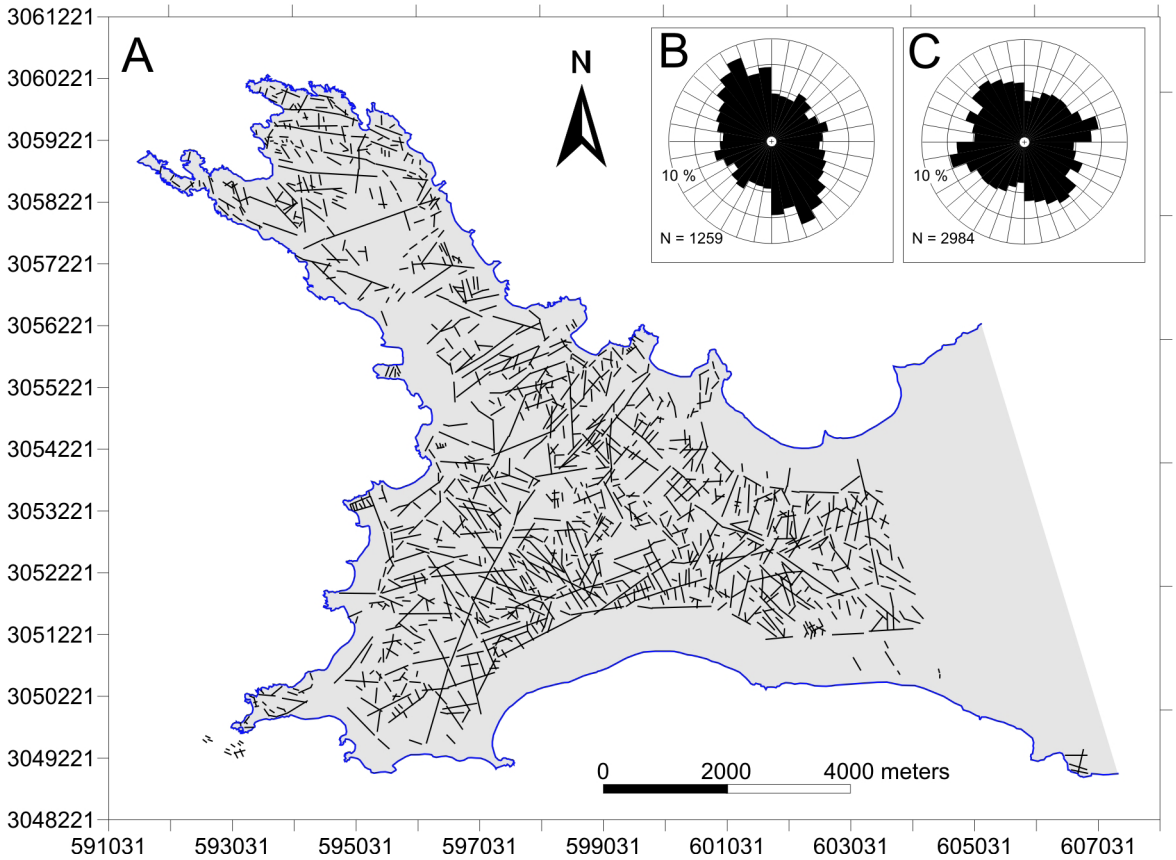

Fig 6.- A) Sketch of the lineaments identified in Byers Peninsula (after López-Martínez *et al.*, 1996a). B) Rose diagram showing the orientation of lineaments in the studied area. C) Rose diagram showing the orientation of lineaments weighting the fracture trace length. N (B and C) is the number of lineaments.

Fig. 6.- A) Lineamientos en la Península Byers (según López-Martínez *et al.*, 1996a). B) Diagrama de rosa de los vientos que muestra la orientación de los lineamientos del área de estudio. C) Diagrama de rosa de los vientos que muestra la orientación de los lineamientos en función de la longitud de fractura. N (B y C) indica el número de lineamientos.

undergone several well defined overprinted stress fields. The determined ellipsoids indicate the presence of extensional and compressional stress regimes. A well defined radial extension is deduced from our paleostress analysis. Also compressional NW-SE to NE-SW paleostress orientations can be deduced from this data set. In stations 4, 6 and 16 the stress ellipsoids have axes with different magnitudes.

4.2. Lineament analysis

From the analysis of the aerial photographs a total of 1,259 lineaments were mapped in Byers Peninsula (Fig. 6A). Rose diagrams represent the orientation of lineaments (Figs. 6B and 6C). To avoid the influence of line-segmentation number, the statistical analysis of fracture directions was made weighting the fracture trace length (Fig. 6C). The length of lineaments varies between 31 m and 1,555 m. Their size distribution is log-normal, with a mode of 100-150 m (Fig. 7A).

Orientation

Lineaments in both igneous and sedimentary rocks in Byers Peninsula show a clear orientation maximum NW-SE, with a dispersion of about 70º (Fig. 7B). This NW-SE trend is also recorded by the direction of the Ray Promontory and some segments of the pre-Holocene terrace scarps in the northern part of the peninsula. Other secondary maxima are NE-SW and ENE-WSW. Although they are not statistically representative when considering the number of lineaments with respect to the main maximum, the secondary sets include several long lineaments in the southern part (ENE-WSW set) and also in the western sector (NE-SW set) of the peninsula, where they control the direction of terrace scarps and of the coast.

The relationship between direction and length (Fig 7C) shows that the most abundant class of lineaments correspond to NW-SE orientations and lengths between 31 and 400 m. NE-SW and ENE-WSW lineaments are dominant at the interval between 400 and longer than 800 m. The

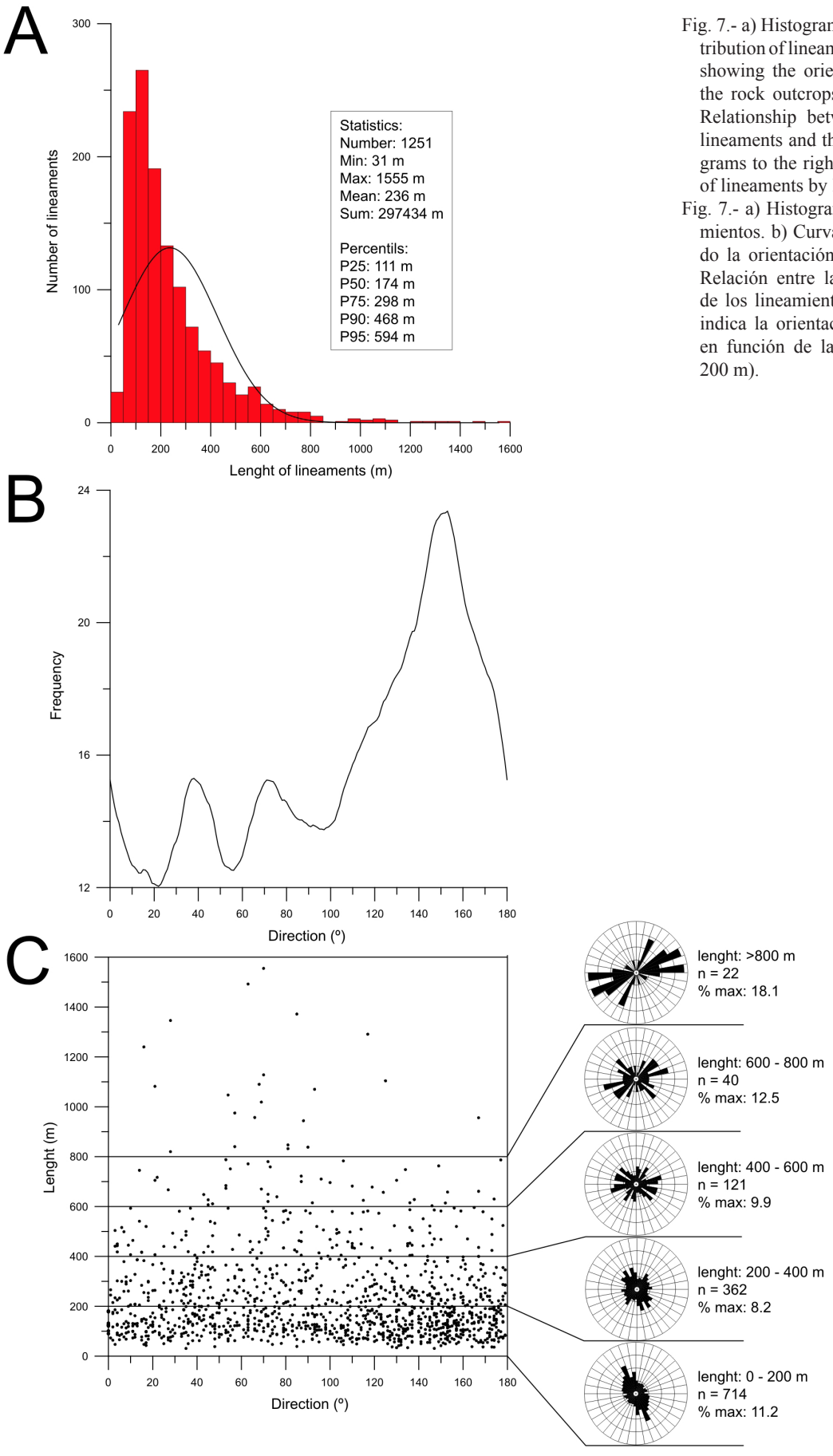

Fig. 7.- a) Histogram showing the length distribution of lineaments. b) Frequency curve showing the orientation of lineaments in the rock outcrops of Byers Peninsula. c) Relationship between the orientation of lineaments and their length. The rose diagrams to the right indicate the orientation of lineaments by length intervals.

Fig. 7.- a) Histograma de longitud de lineamientos. b) Curva de frecuencia mostrando la orientación de los lineamientos. c) Relación entre la orientación y longitud de los lineamientos. El diagrama en rosa indica la orientación de los lineamientos en función de la longitud (intervalos de 200 m).

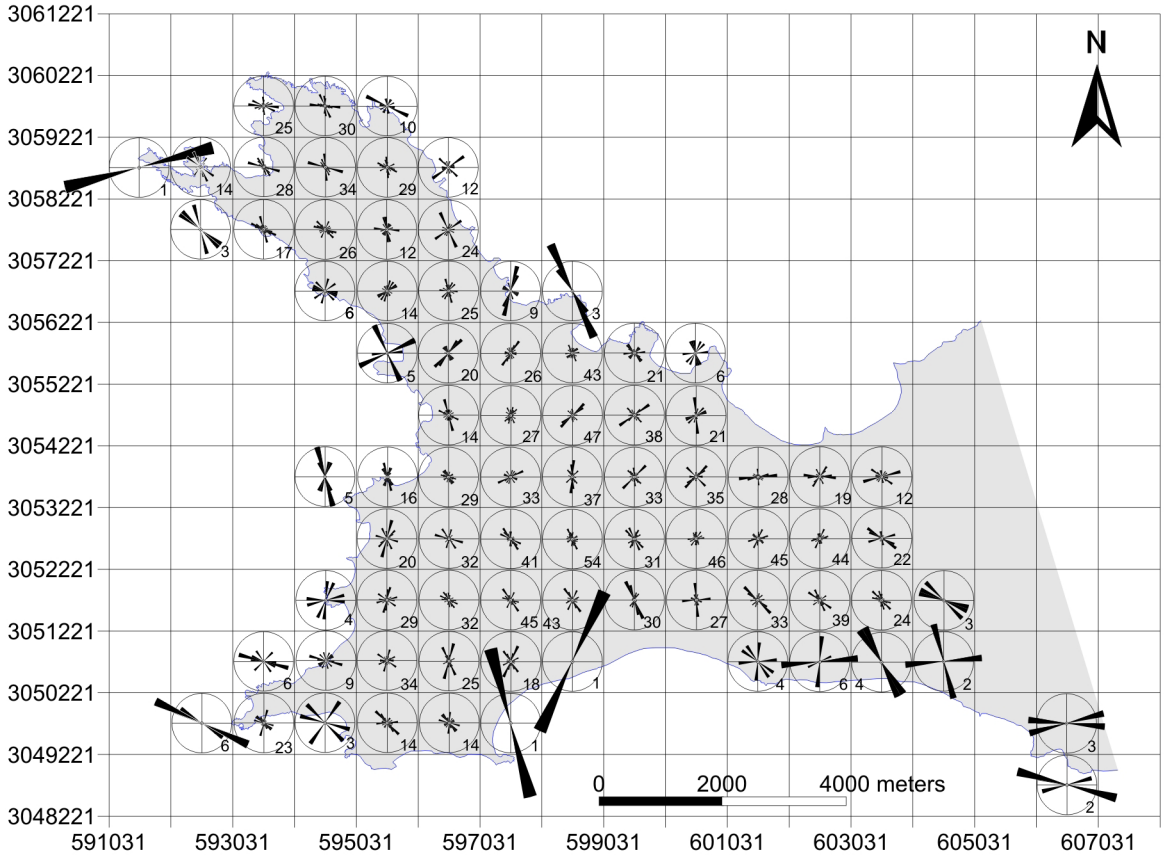

Fig 8.- Lineament distribution variations across the studied area by means of square cell grid (1 km x 1 km). Outer circles in the rose diagrams represent 40% of data.

Fig. 8.- Variación en la distribución de lineamientos a lo largo del área de estudio con una malla cuadrada de celdas de 1x1 km. Los círculos externos de los diagramas en rosa representan el 40% de los datos.

NE-SW lineaments represent a secondary maximum in the 200-400 m interval. An aspect of length-orientation relationships is that NE-SW and ENE-WSW lineaments are increasingly important when considering longer lineaments.

Spatial variations in the orientation of lineaments were calculated by means of a grid of square cells, representing the length and number of lineaments in each cell (Fig. 8).The results show a consistent pattern of dominant NW-SE directions, with secondary maxima similar to those obtained in the analysis of total data. Overall, the maximum NW-SE direction is in the northwestern part of Byers Peninsula, in the Ray Promontory (between horizontal reference lines 3060221 and 3057221 and between vertical reference lines 592031 and 596031); and in the southern sector (between horizontal reference lines 3053221 and 3049221 and between vertical reference lines 592031 and 604031, Fig. 8). In the southern part of the Peninsula NE to ENE direction becomes prevalent (between horizontal reference lines 3057221 and 3053221 and between vertical reference lines 595031 and 604031, Fig. 8). Occasionally, for example in the southwestern part of the Peninsula, both directions are present with the same frequency.

Density

In the study area, the mean average distance between lineaments in igneous and sedimentary rocks in Byers Peninsula is 292 m (Fig 9A), and the mode about 150 m, very similar to the mode for lineaments length (see Figs. 7A and 9A). The cumulative percentage Φ_{95} is about 600 m. The contour map of distance between lineaments shows that, in most parts of the study area, the distance between lineaments varies between 36 and 300 m (Fig 9B). To construct a density map with geological significance, the minimum cell size must be greater than the distance between fractures previously calculated (Cortés *et al.,* 2003).

To calculate lineament density, several tests were made, with cells of different sizes. When the cell size is too small (100 m x 100 m), the contour map is not more representative than the lineaments map, since many null values appear. We chose a cell size of 1000 m x 1000 m (between four and five times the average spacing of lineaments) in

order to show an outcrop-scale map with geological significance (Fig. 7). This implies that reasonable accuracy is achieved and cell with null values between lineaments are avoided.

The fracture density in the peninsula show several minima due to recent to modern beach deposits, stone fields or debris slope processes which cover the rock outcrops. The fracture density maxima within the exposed outcrops are variously located (Fig. 10): (i) near of the northwestern margin of the Ray Promontory, (ii) at the south of Punta Varadero and Chester Cone and (iii) at the north of Cerro Negro, following a WNW-ESE shape.

5. Discussion: Recent evolution of the South Shetland Block from morphostructural and paleostress analyses

By integrating morphostructural results with those obtained from the paleostress analysis we can compare previously published data from the region, and then fit these into regional geodynamic models.

5.1. Comparison between the local and regional stress fields

Several paleostress analyses were previously made in different parts of the South Shetland Block and surrounding areas. In Hurd Peninsula (Livingston Island) several authors deduce a NW-SE extensional regime (Santanach *et al.*, 1992; Sàbat *et al.*, 1992; Willan, 1994; González-Casado *et al.*, 1999). Prior to this extensional regime, two orientations of σ1 were deduced corresponding to a wrench-faulting regime. In King George Island, a similar stress field was defined by Smellie *et al.* (1984), Tokarski (1991) and Uhlein *et al.* (1993). Galindo-Zaldívar *et al.* (2006) and López-Martínez *et al.* (2006) studied recent tectonics of Elephant Island. According to these authors,

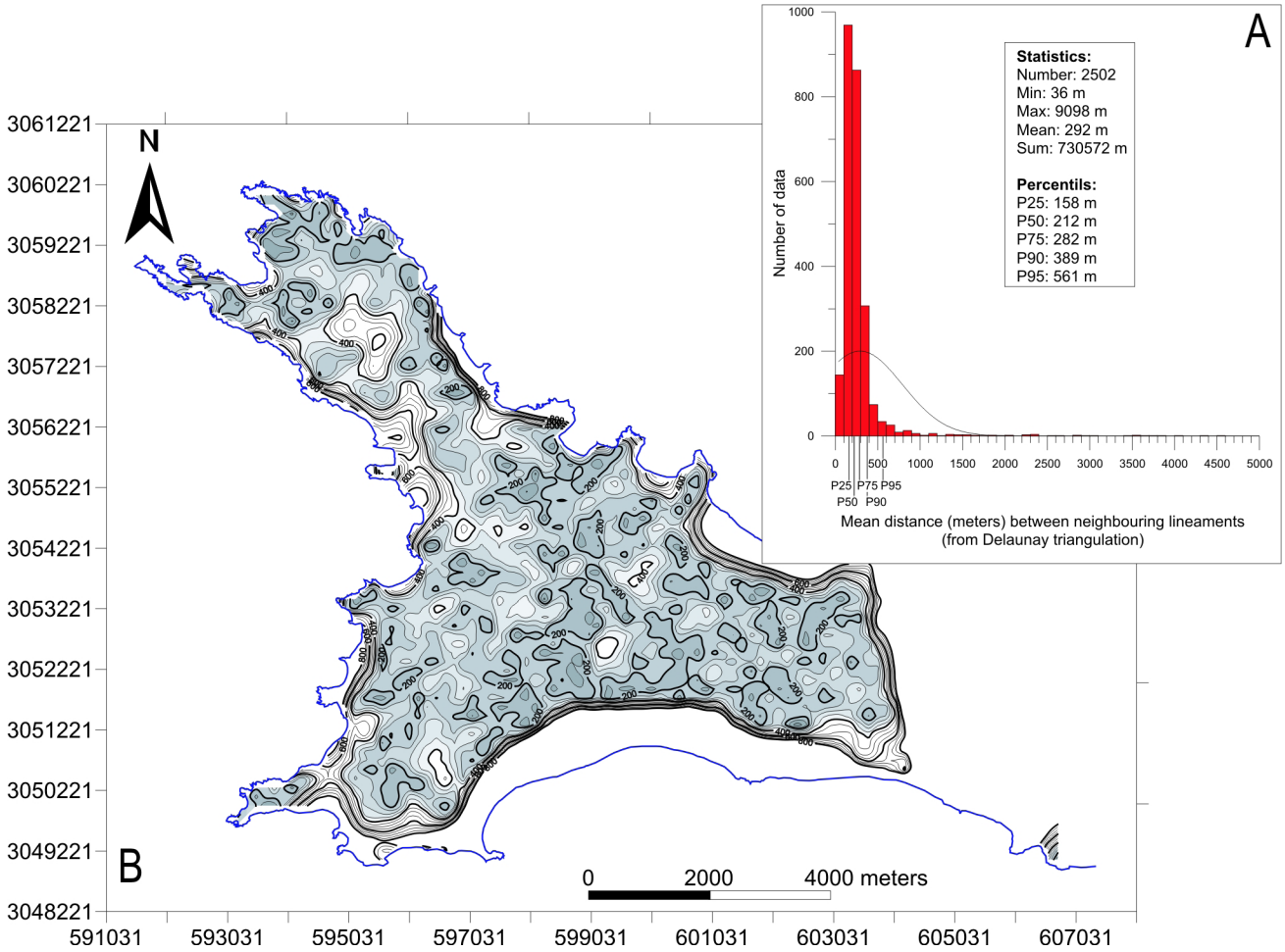

Fig. 9.- A) Histogram of the calculated distances based on Delaunay triangulation. B) Contour map of average distances between lineaments in the rock outcrops of Byers Peninsula. Isoline values represent distance in meters. Grey areas indicate average distance between fractures less than 350 m.

Fig. 9.- A) Histograma de las distancias calculadas en base a la triangulación de Delaunay. B) Mapa de contornos de la distancia media entre lineamientos de la Península Byers. Las isolíneas representan distancia en metros. Las áreas de color gris indican distancias entre fracturas de menos de 350 m.

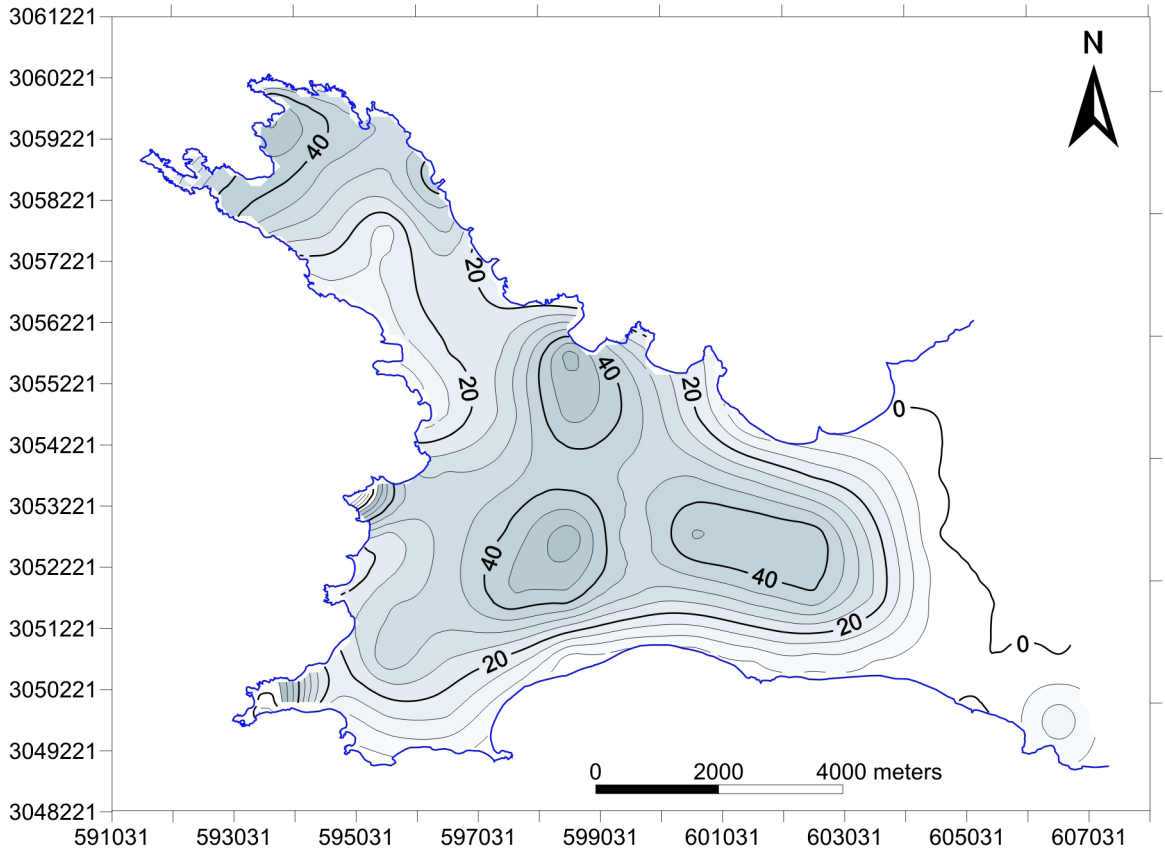

Fig 10.- Fracture density contour map. Isoline values represent density calculated as length of lineaments per square meter using a grid of square cells of 1 km x 1 km.

Fig. 10.- Mapa de contornos de la densidad de lineamientos. Las isolíneas representan la longitud de lineamientos por metro cuadrado usando una malla con celdas de 1x1 km.

the northwestern sectors are dominated by NE-SW and NW-SE compression, related to the Scotia-Antarctica left-lateral movement and to the subduction of oceanic lithosphere. The southern sector is characterized by WNW-ESE extension related to the opening of the Bransfield Basin. Maestro *et al.* (2007) deduced on Deception Island a recent stress field characterized by NE-SW and WNW-ESE to NW-SE extension, with local compression with NW-SE and NNE-SSW to NE-SW maximum horizontal orientations.

Our paleostress data, from brittle mesostructures at Byers Peninsula, show many sites (1, 8, 12, 13, 14, 15) with a vertical well odd axis, that probably corresponds to σ_1. This supports a stage of regional extension related to the uplift of the South Shetland Block. Additionally, E-W to NE-SW odd axes were identified in many sites from the northeast (3, 14), central (2), south (5, 6, 12) and northwest (16). This corresponds to a major regional stress field that was active in the region. These ellipsoids probably represent a NE-SW compression related to the convergence of the Scotia-Antarctic plates. The western coast of Byers Peninsula is characterized by very consistent NW-SE odd axes. These may represent a NW-SE compressive stage related to the relative westward motion of the South Shetland Block in respect to the Antarctic Peninsula, or a local perturbation of the E-W oriented compressive field. Finally, N-S compression is observed in several stations (1, 11) that may be associated with subduction activity along the South Shetland Trench.

Dispersion of maximum horizontal stress trajectories is interpreted as the product of local perturbations in this regional stress field related to the nearby Hero Fracture Zone, and its interaction with several geodynamic processes acting in the region.

5.2. Relationship between density of lineaments in Byers Peninsula and the underlaying structures

The dominant orientations of lineaments are consistent with the orientation of dykes and faults measured in Byers Peninsula by Valenzuela and Hervé (1972) and Smellie *et al.* (1984). Fault and joints measured at these 16 stations show a large dispersion, but the NW-SE orientation predominates. Also, these fractures show NE-SW

and E-W secondary maximums.

The lineament density variation in the studied area can be correlated with the underlying macrostructures involving igneous and sedimentary rocks. This relationship is especially noticeable in the central and eastern parts of Byers Peninsula, where there are two lineament density maxima in N-S and WNW-ESE direction. They could be related with the extension of N-S to transfer zones that divided the Bransfield Basin (Jeffers *et al.,* 1991; Maestro *et al.,* 2007) and with the main trend of Livingston Island uplift from oblique convergence between the Antarctic and Pacific plates (González-Casado *et al.,* 2000; Maestro *et al.,* 2007). This means that fracturing of rocks, even with different orientation, is pervasive near the large structures underlaying the studied area. The explanation for this effect may lie in the role of large structures as inhomogeneities and 'stress raising zones' (Pollard and Segall, 1987; Sassi *et al.,* 1993; Sassi and Faure, 1997).

6. Conclusions

The tectonic imprint of recent geodynamic processes in Mesozoic rocks of Byers Peninsula is deduced from the analysis of lineaments and brittle mesostructures, which are overprinted on prior stress regimes. Lineaments, which show similar trends to fractures, are related to the underlying macrostructures developed in igneous and sedimentary rocks.

Palaeostress analysis at Byers Peninsula indicates that the area has undergone radial to NNW-SSE to NNE-SSW extension, and local compressions in a NE-SW and NW-SE direction, which are in agreement with other results obtained by several research groups in the region.

The integrated study of paleostress data from the South Shetland Block and its surrounding areas indicates several stress sources: (1) the recent stress field characterized by NNW-SSE to NNE-SSW extension, related to the opening of the backarc Bransfield Basin, (2) NE-SW maximum horizontal stress field is related to the left-lateral displacement between the Antarctica and Scotia plates, and (3) NW-SE to N-S compression is related to the oceanic lithosphere subduction under the Antarctic plate along the South Shetland Trench. Perturbations of the maximum horizontal stress trajectories are produced by the Hero and Shackleton fracture zones. In addition, structural and lithological heterogeneities produce local dispersions of these orientations.

Acknowledgements

Financial support for this work was provided by the research projects REN2001-0643, CGL2005-03256 and CGL2007-28812-E/ANT of the Spanish R & D National Plan. The authors thank to the colleagues and logistic personnel that provided support for the field work. The cooperation of the Limnopolar project directed by Dr. A. Quesada is specially appreciated. We also thank Drs. Moratti and Arche for their useful comments.

References

Araya, R., Hervé, F. (1966): *Estudio geomorfológico y geológico en las Islas Shetland del Sur, Antártida*. Instituto Antártico Chileno Publicación, 8: 76 p.

Ashcroft, W.A. (1972): *Crustal structure of the South Shetland Islands and Bransfield Strait*. British Antarctic Survey Scientific Reports, 66: 43 p.

Barker, P.F., Dalziel, I.W.D., Storey, B.C. (1991): Tectonic development of the Scotia Arc region. In: R.J. Tingey (ed.), *Antarctic geology*. Oxford, U.K., Oxford University Press: 215-248.

Casas, A.M., Cortés, A.L., Maestro, A., Soriano, M.A., Riaguas, A., Bernal, J. (2000): LINDENS: a basic program for lineament analysis. *Computer Geosciences,* 26: 1011-1022.

CGE-UAM-BAS (1992): *Topographic Map of Byers Peninsula, E. 1:25.000*. Spanish Antarctic Cartography, Centro Geográfico del Ejército, Madrid.

Cortés, A.L., Soriano, M.A., Maestro, A., Casas, A.M. (2003): The role of tectonic inheritance in the development of recent fracture systems, Duero Basin, Spain. *International Journal Remote Sensing,* 24: 4325-4345.

Covacevich, V. (1976): Fauna valanginiana de Península Byers, Isla Livingston, Antártica. *Revista geológica de Chile*, 3: 25-56.

Crame, J.A., Pirrie, D., Crampton, J.S., Duane, A.M. (1993): Stratigraphy and regional significance of the Upper Jurassic-Lower Cretaceous Byers Group Livingston Island, Antarctica. *Journal of the Geological Society*, 150: 1075-1087.

Dalziel, I.W.D. (1983): The evolution of the Scotia Arc: a review. In: R.L. Oliver, P.R. James, J.B. Jago (eds.), *Antarctic Earth Science*. Cambridge University Press, UK: 288-293.

Davey, F.J. (1972): Marine gravity measurements in Bransfield Strait and adjacent areas. In: R.J. Adie (ed.), *Antarctic geology and geophysics.* Oslo, Universitetsforlaget: 39-46.

Demant, A., Touron, S., Lapierre, H., Bosch, D. (2004): Cretaceous arc volcanism of Byers Peninsula, Livingston Island, Antarctica: new petrological, geochemical and isotope data. *Bulletin de la Societé Géologique de France*, 175, 2: 131-145.

Dietrich, R., Dach, R., Engelhardt, G., Heck, B., Kutterer, H., Lindner, K., Mayer, M., Menge, F., Mikolaiski, J.W., Niemeier, W., Pohl, M., Salbach, H., Schenke, H.W., Schöne, T., Seeber, G., Soltau, G. (1996): The SCAR 95 GPS Campaign: obtectives, data analysis and final solution. In: R. Dietrich (ed.), *The Geodetic Antarctic Project GAP95 German Contributions to the SCAR 95 Epoch Campaign*. Deutsche Geodätische Kommission bei der Bayerischen Akademie der Wissenschaften, Reithe B, Heft 304, München: 9-14.

Dietrich, R., Dach, R., Engelhardt, G., Ihde, J., Korth, W., Kutterer, H., Lindner, K., Mayer, M., Menge, F., Miller, H., Müller, C., Niemeier, W., Perlt, J., Pohl, M., Salbach, H., Schenke, H.W., Schöne, T., Seeber, G., Veit, A., Völksen, C. (2001): ITRF coordinates and plate velocities from repeated GPS campaigns in Antarctica. An analysis based on different individual solutions. *Journal of Geodesy*, 74: 756-766.

Galindo-Zaldívar, J., Maestro, A., López-Martínez, J., Sanz de Galdeano, C. (2006): Elephant Island recent tectonics in the framework of the Scotia-Antarctic-South Shetland Block triple junction (NE Antarctic Peninsula). In: Fütterer, D.K., Damaske, D., Kleinschmidt, G., Miller, H., Tessensohn, F. (eds.), *Antarctic Contributions to Global Earth Science.* Springer, Berlin-Heildelberg-New York: 271-276.

Galindo-Zaldívar, J., Gamboa, L., Maldonado, A. (2004): Tectonic development of the Bransfield Basin and its prolongation to the South Scotia Ridge, northern Antarctic Peninsula. *Marine Geology*, 206: 267-282.

Galindo-Zaldívar, J., Jabaloy, A., Maldonado, A., Sanz de Galdeano, C. (1996): Continental fragmentation along the South Scotia Ridge transcurrent plate boundary. *Tectonophysics*, 259: 275-301.

Galindo-Zaldívar, J., González-Lodeiro, F. (1988): Faulting phase differentiation by means of computer search on a grid pattern. *Annales Tectonicae*, 2: 90-97.

Gamboa, L.A.P., Maldonado, P.R. (1990): Geophysical investigations in the Bransfield Strait and in the Bellingshausen Sea, Antarctica. In: B. St. John (ed.), *Antarctica as an Exploration Frontier-Hydrocarbon Potential, Geology and Hazards*. Am. Assoc. Petr. Geology, 31: 127-141.

González-Casado, J.M., Giner, J.L., López-Martínez, J. (1999): La fracturación en el Cabo Shirreff, Isla Livingston, Antártida Occidental. *Geogaceta*, 26: 31-34.

González-Casado, J.M., Giner, J.L., López-Martínez, J. (2000): Bransfield Basin, Antarctic Peninsula: Not a normal backarc basin. *Geology*, 28: 1043-1046.

González-Casado, J.M., López-Martínez, J., Durán, J.J. (1999): Active tectonics and morphostructure at the northern margin of the Central Bransfield Basin, Hurd Peninsula, Livingston Island (South Shetland Islands). *Antarctic Science*, 11: 323-331.

González Ferrán, O. (1991): Volcanic and tectonic evolution of the Northern Antarctic Peninsula, Late Cenozoic to recent. *Tectonophysics*, 114: 389-409.

González Ferrán, O., Katsui, Y., Tavera, J. (1970): Contribución al conocimiento geológico de la Península Byers de la Isla Livingston: Islas Shetland del Sur, Antártica. *Instituto Antártico Chileno*, *Serie Científica*, 1: 41-54.

Hathway, B., Lomas, S.A. (1998): The Upper Jurassic-Lower Cretaceous Byers Group, South Shetland Islands, Antarctica: revised stratigraphy and regional correlations. *Cretaceous Research*, 19, 1: 43-67.

Hernández, P.J., Azcárate, V. (1971): Estudio paleobotánico preliminar sobre restos de una tafoflora de la Península Byers (Cerro Negro), Isla Livingston, Islas Shetland del Sur, Antártica. *Instituto Antártico Chileno, Serie Científica*, 2: 15-50.

Hobbs, G.J. (1968): The geology of the South Shetland Islands: IV. The Geology of Livingston Island. *British Antarctic Survey Scientific Reports*, 47: 34 p.

Jeffers, J.D., Anderson, J.B., Lawver, L.A. (1991): Evolution of Bransfield basin, Antarctic Peninsula. In: M.R.A. Thomson, J.A. Crame., J.W. Thomson (eds.), *Geological evolution of Antarctica*. Cambridge University Press, Cambridge, UK: 481-485.

Klepeis, K.A., Lawver, L.A. (1996): Tectonics of the Antarctic-Scotia plate boundary near Elephant and Clarence islands, West Antarctica. *EOS (Trans. Am. Geophys. Union)*, 73: 563.

Larter, R.D., Barker, P.F. (1991): Effects of ridge crest-trench interaction on Antarctic-Phoenix spreading: forces on a young subducting plate. *Journal of Geophysical Research*, 96: 19586-19607.

Lawver, L.A., Sloan, B.J., Barker, D.H.N., Ghidella, M., Von Herzen, R.P., Keller, R.A., Klinkhammer, G.P., Chin, C.S. (1996): Distributed, active extension in Bransfield Basin, Antarctic Peninsula: Evidence from multibeam bathymetry. *GSA Today*, 6: 1-16.

Lawver, L.A., Keller, R.A., Fisk, M.R., Strelin, J. (1995): Bransfield Strait, Antarctica Peninsula: Active extension behind a dead arc. In: B. Taylor (ed.), *Back-arc Basins: Tectonics and Magmatism*. Plenum Publishing Corporation, New York: 315-342.

López-Martínez, J., Martínez de Pisón, E., Serrano, E., Arche, A. (1995): *Geomorphological Map of Byers Peninsula. E. 1:25.000.* BAS Geomap Series. British Antarctic Survey, Cambridge, UK.

López-Martínez, J., Trouw, R.A.J., Galindo-Zaldívar, J., Maestro, A., Simoes, L.S.A., Medeiros, F.F., Trouw, C.C. (2006): Tectonics and geomorphology of Elephant Island, South Shetland Islands. In: Fütterer, D.K., Damaske, D., Kleinschmidt, G., Miller, H., Tessensohn, F. (eds.), *Antarctic Contributions to Global Earth Science.* Springer, Berlin-Heildelberg-New York: 277-281.

López-Martínez, J., Hathway, B., Lomas, S., Martínez de Pisón, E., Arche, A. (1996a): Structural geomorphology and geological setting. In: J. López-Martínez, M.R.A. Thomson, J.W. Thomson (eds.), *Supplementary text of the Geomorphological map of Byers Peninsula, Livingston Island*. BAS Geomap Series, 5-A. Cambridge, UK: 9-14.

López-Martínez, J., Thomson, M.R.A., Thomson, J.W. (Eds.) (1996b): Geomorphological Map Byers Peninsula, Livingston Island. *Supplementary text of the Geomorphological map of Byers Peninsula, Livingston Island*. BAS Geomap Series, 5-A. Cambridge, UK: 65 p.

Maestro, A., Somoza, L., Rey, J., Martinez-Frías, J., López-Martínez, J. (2007): Active tectonics, fault patterns and stress field of Deception Island: A response to oblique convergence between the Pacific and Antarctic plates. *Journal of South American Earth Sciences*, 23, 2-3: 256-268.

Maldonado, A., Larter, R.D., Aldaya, F. (1994): Forearc tectonic evolution of the South Shetland Margin, Antarctic Peninsula. *Tectonics*, 13: 1345-1370.

Pankhurst, R.J., Weaver, S.D., Brook, M., Saunders, A.D. (1979): K-Ar chronology of Byers Peninsula, Livingston Is-

land, South Shetland Islands. *British Antarctic Survey Bulletin*, 49: 277-282.

Pelayo, A., Wiens, D. (1989): Seismotectonics and relative plate motions in the Scotia Sea region. *Journal of Geophysical Research*, 94: 7293-7320.

Pollard, D.D., Segall, P. (1987): Theoretical displacements and stresses near fractures in rock, with application of faults, joints, veins, dikes, and solution surfaces. In: B.K. Atkinson (ed.), *Fracture Mechanism of Rock*: 277-349.

Preparata, F.P., Shamos, M.I. (1985): *Computational Geometry: An Introduction*. Springer-Verlang, New York.

Rey, J., Somoza, L., Martínez-Frías, J. (1995): Tectonic, volcanic and hydrothermal event sequence on Deception Island (Antarctica). *Geo-Marine Letters*, 15: 1-8.

Sàbat, F., Serrat, D., Vilaplana, J.M. (1992): Cenozoic tectonic evolution in Livingston Island (South Shetland, Antarctica): Mesostructural and geomorphological approach. *Revista de la Sociedad Geológica de España*, 5: 159-166.

Santanach, R., Pallàs,, F., Sàbat, F., Muñoz, J.A. (1992): La fracturación en la Isla Livingston, Islas Shetland del Sur. In: J. López-Martínez (ed.), *Geología de la Antártida Occidental. III Congreso Geológico de España*, Salamanca, Spain, Simposios, 3: 141-151.

Sassi, W., Colletta, B., Balé, P., Paquereau, T. (1993): Modelling of structural camplexity in sedimentary basins: the role of pre-existing faults in thrust tectonics. *Tectonophysics*, 226: 97-112.

Sassi, W., Faure, J.L. (1997): Role of faults and layer interfaces on the spatial variation of stress regimes in basins: inferences from numerical modelling. *Tectonophysics*, 266: 101-119.

Sell, I., Poupeau, G., González-Casado, J.M., López-Martínez, J. (2004): A fission track thermochronological study of King George and Livingston Islands, South Shetland Islands (West Antarctica). *Antarctic Science*, 16 (2): 191-197.

Smellie, J.L., Pankhurst, R.J., Thomson, M.R.A., Davies, R.E.S. (1984): *The geology of the South Shetland Islands: VI. Stratigraphy, geochemistry and evolution.* British Antarctic Survey Scientific Reports, nº 87.

Smellie, J.L., Davies, R.E.S., Thomson, M.R.A. (1980): Geology of a Mesozoic intra-arc sequence on Byers Peninsula, Livingston Island, South Shetland Islands. *British Antarctic Survey Bulletin*, 50: 55-76.

Solari, M.A., Hervé, F., Martinod, J., Le Roux, J.P., Ramírez, L.E., Palacios, C. (2008): Geotectonic evolution of the Bransfield Basin, Antarctic Peninsula: insights from analogue models. *Antarctic Science*, 20 (2): 185-196.

Tavera, J. (1970): Fauna Titoniana-Neocomiana de la Isla Livingston, Islas Shetland del Sur, Antártica. *Instituto Antártico Chileno, Serie Científica*, 1: 175-186.

Tokarski, A.K. (1991): The Late Cretaceous-Cenozoic structural history of King George Island, South Shetland Islands, and its plate-tectonic setting. In: M.R.A. Thomson, J.A. Crame, J.W. Thomson (eds.), *Geological Evolution of Antarctica*. Cambridge University Press, Cambridge: 417-422.

Uhlein, A., Trompette, R.R., Rocha-Campos, A.C., Dos-Santos, P.R., Gipp, M., Simöes, J.C. (1993): Regime compresivo atrás de una zona de subducçao: juntas subhorizontais no arco magmático cenozoico da Ilha Rei George. *IV Simp. Bras. Geol., Soc. Bras. Geol. Nucleo Minas Gerais*, 12: 330-339.

Valenzuela, E., Hervé, F. (1972): Geology of Byers Peninsula, Livingston Island, South Shetland Islands. In: R.J. Adie (ed.), *Antarctic geology and geophysics*, Universitetsforlaget, Oslo: 83-89.

Wallace, R.E. (1951): Geometry of shearing stress and relation to faulting. *Journal of Structural Geology*, 59: 118-130.

Willan, R.C.R. (1994): Structural setting and timing of hydrothermal veins and breccias on Hurd Peninsula, South Shetland Islands: a possible volcanic-related epithermal system in deformed turbidites. *Geological Magazine*, 131: 465-483.